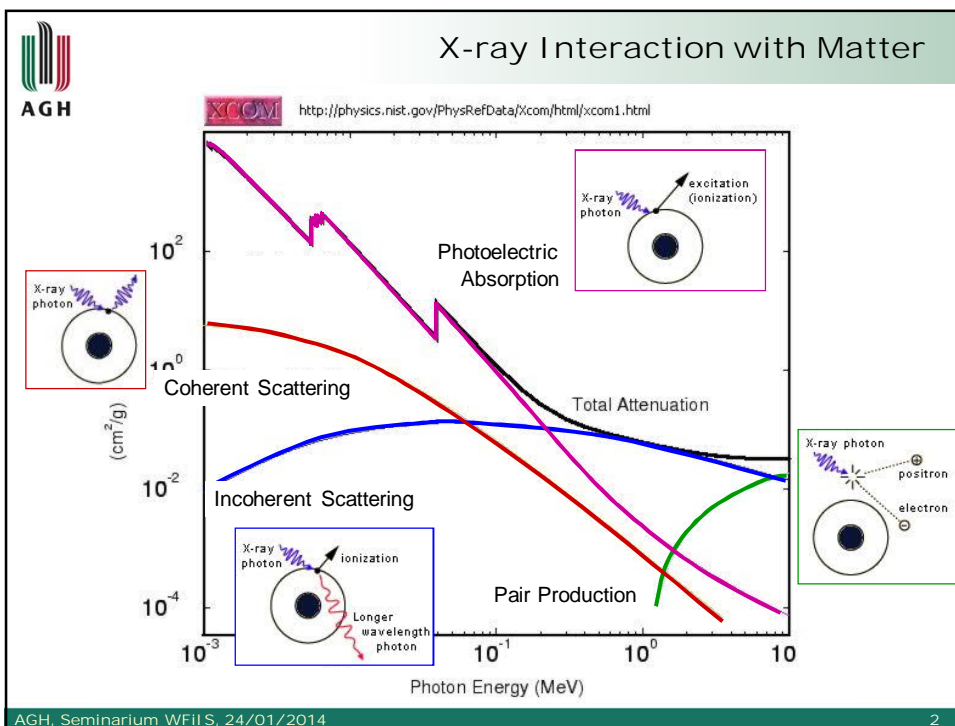


Wysokorozdzielcza spektroskopia rentgenowska

HERFD-XAS: high energy resolution fluorescence detected X-ray absorption spectroscopy

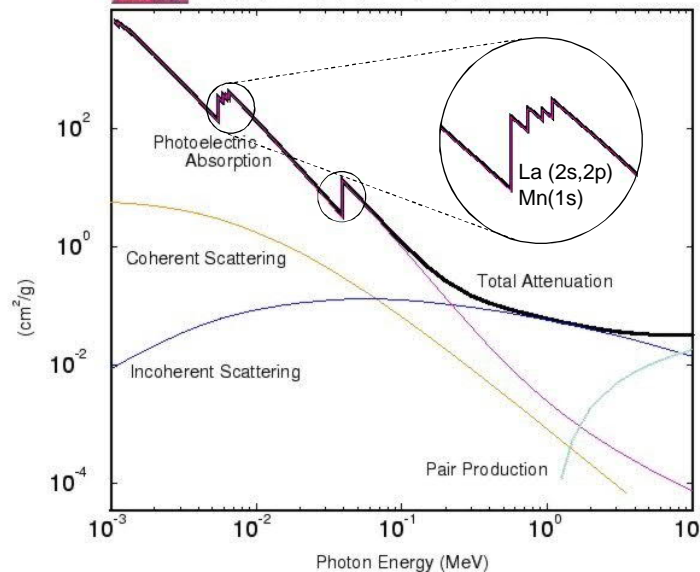
(R)XES: (resonant) X-ray emission spectroscopy

RIXS: resonant inelastic X-ray scattering



Resonant X-ray absorption

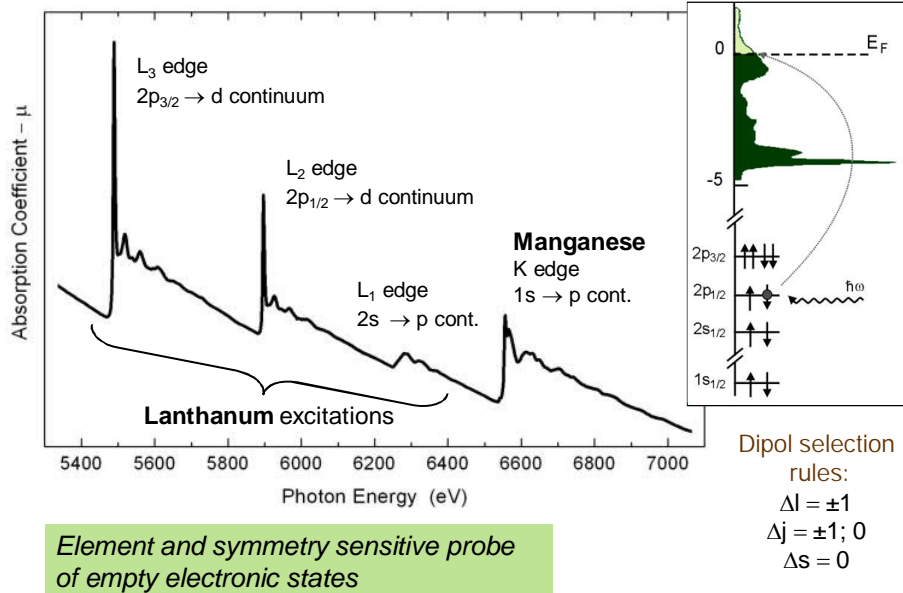
XCOM <http://physics.nist.gov/PhysRefData/Xcom/html/xcom1.html>



AGH, Seminarium WFiIS, 24/01/2014

3

X-ray absorption spectroscopy (XAS)



AGH, Seminarium WFiIS, 24/01/2014

4

X-ray absorption spectroscopy (XAS)

TM:K edge
1s → p (d) cont.

Pre-edge structure:
quadrupolar excitations
(e.g. 1s → d cont.)
✓ p-d hybridisation
→ crystal field multiplets

Near edge structure: $\mu(E) \sim |M_{hf}|^2 \rho(E)$
Broadened DOS of the electronic states above E_F

Extended range fine structure (EXAFS)
Oscillations due to interference of outgoing and
(multiple) scattered photoelectron wave
Local symmetry → number of NN, PDF

Edge energy:
Fermi level with respect to core levels
✓ chemical shift → valence state
✓ static probe: $\tau \sim 10^{-14} s$

AGH, Seminarium WFiS, 24/01/2014

5

X-ray absorption spectroscopy (XAS)

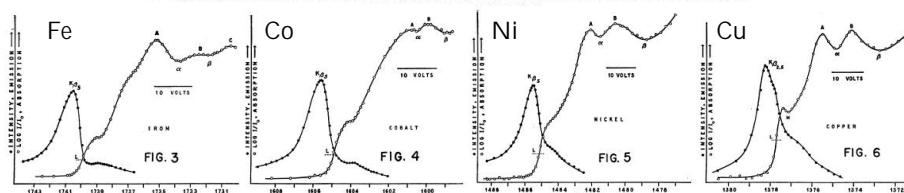
SEPTEMBER 1, 1939

PHYSICAL REVIEW

VOLUME 56

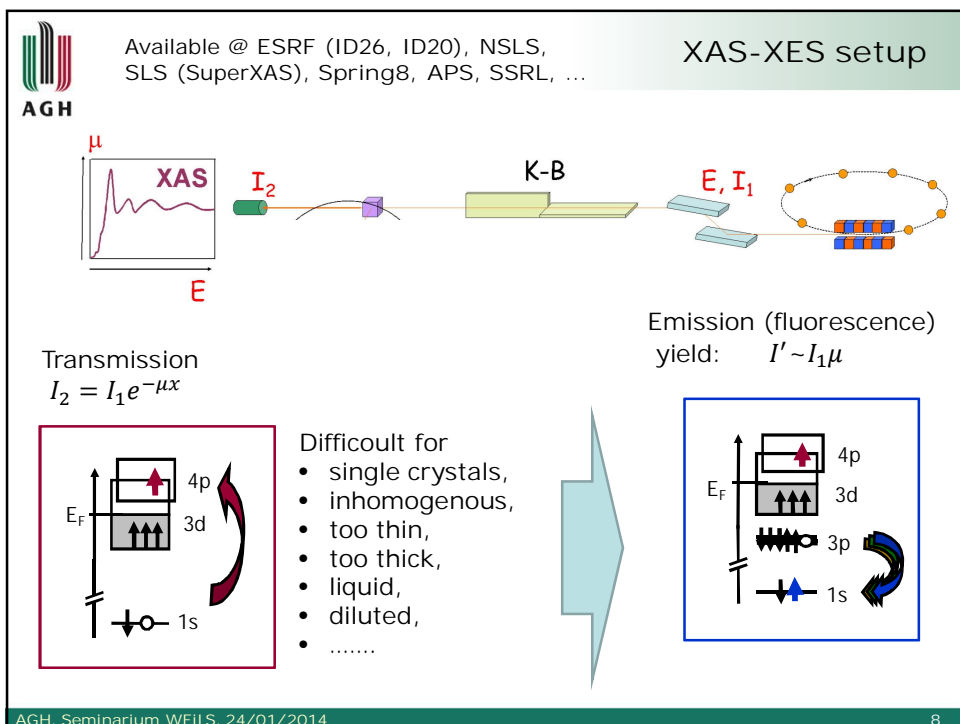
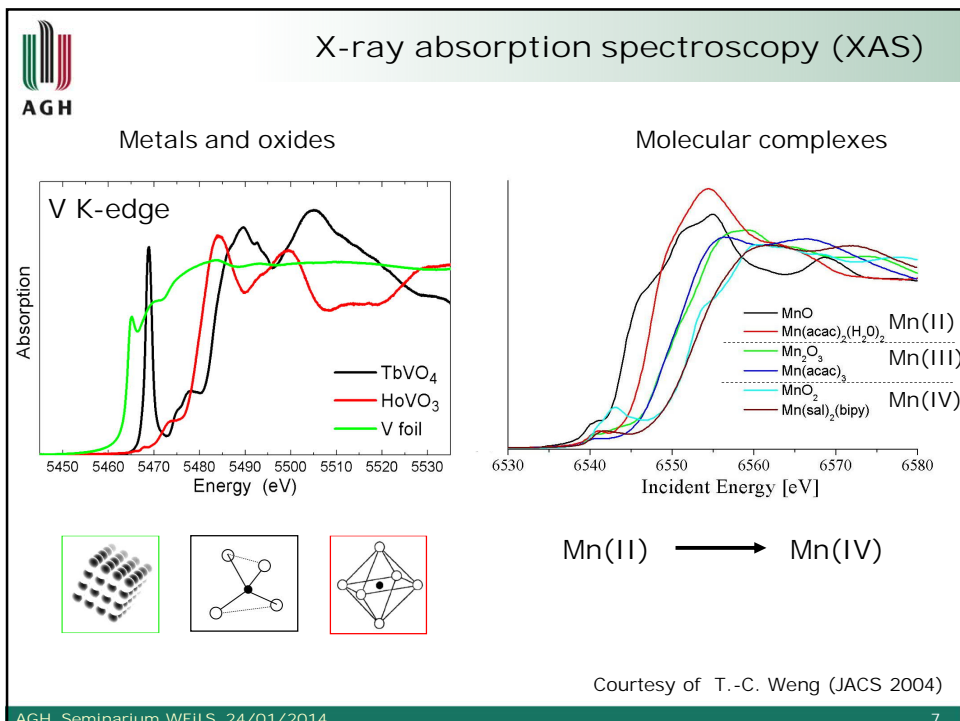
The X-Ray K Absorption Edges of the Elements Fe (26) to Ge (32)

W. W. BEEMAN AND H. FRIEDMAN
Rowland Physical Laboratory, The Johns Hopkins University, Baltimore, Maryland



AGH, Seminarium WFiS, 24/01/2014

6



 The European Synchrotron



A LIGHT FOR SCIENCE



ESRF Members and their share of the budget

- 27.5% France
- 25.5% Germany
- 15% Italy
- 14% United Kingdom
- 4% Spain
- 4% Switzerland
- 6% Benesync (Belgium, The Netherlands)
- 4% Nordsync (Denmark, Finland, Norway, Sweden)

Additional contributions

- 1% Portugal
- 1% Israel
- 1% Austria
- 1% Poland
- 1.05% Centralsync (Czech Republic, Hungary, Slovakia)
- 0.3% South Africa

AGH, Seminarium WFIIS, 24/01/2014

9

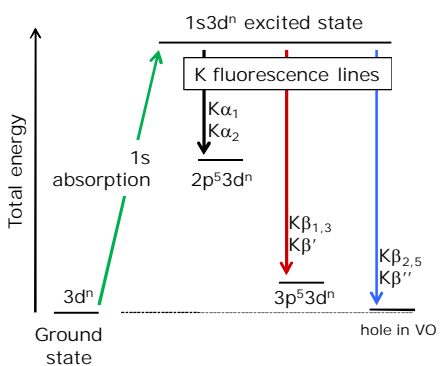
 Take a breath for acknowledgements

Cz. Kapusta, K. Kollbek, J. Stępień, A. Kozłowski AGH	M. Zająć Solaris, UJ
P. Glatzel, B. Gorges, S. Eeckhout, K. Kvashnina, J. Swabrick-Grattage ESRF, Grenoble	T.-C. Weng, R. Alonso Mori SSRL, Stanford
O. Safonova, J. Szlachetko, J. Sa SLS, PSI, Villigen	D. Koziej ETH, Zurich
A. Juhin, Ph. Sainctavit IMPMC, Université Pierre et Marie Curie, Paris	G. Vankó KFKI, Budapest
K. Knížek, Z. Jirák Institute of Physics CAS, Prague	V. Prochazka Olomouc University
M. Balden, C. Adelhelm MPI für Plasmaphysik, Garching	W. Szczerba BAM, Berlin
G. Simon, L. Morellon, R. Ibarra INA, Universidad de Zaragoza	M. Kavčič JSI, Ljubljana

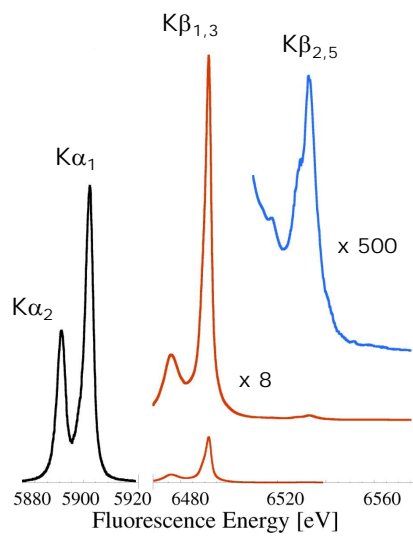
AGH, Seminarium WFIIS, 24/01/2014

10

Simillar information as in XPS,
but for (diluted, insulating, buried ...)
bulky samples

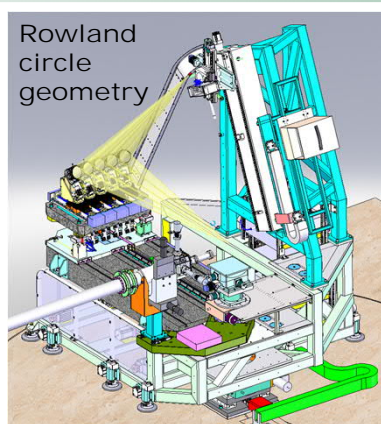


K emission lines



X-ray emission (fluorescence) detection

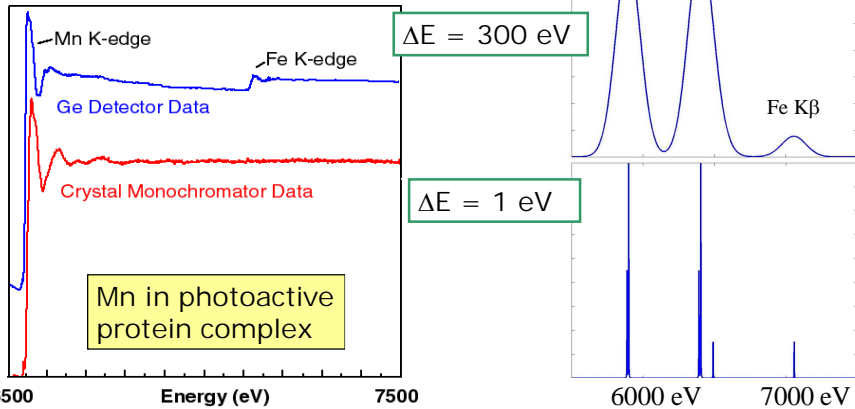
Energy Bandwidth	
Photodiode	n/a
Ge detector	200 eV
Si drift detect	130 eV
Bent Cryst Laue An	50 eV
Bent Crystal Bragg Analyzers	1-2 eV
	< 0.5 m Spectrometer
0.6-1.0 eV	1 m Spectrometer
~ 0.3 eV	2 m Spectrometer



High deadtime at SR sources: ☹

Why do we need high resolution?

- instead of
- high solid angle
 - large energy range



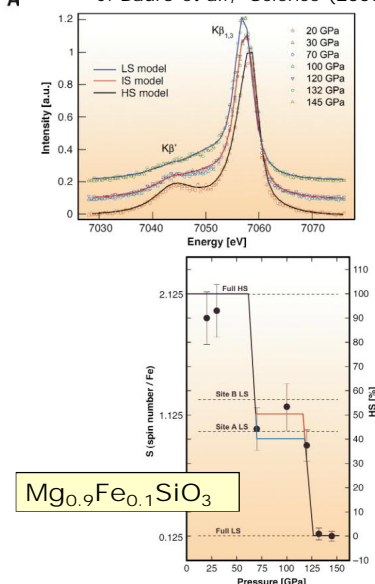
Courtesy of P. Glatzel

AGH Seminarium WFIIS, 24/01/2014

13

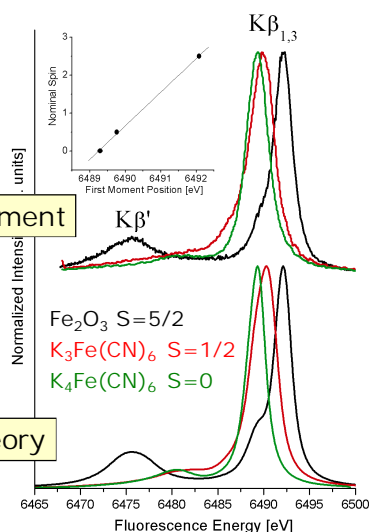
Spin sensitivity of K β main line

J. Badro et al., Science (2003 & 2004)



Experiment

Theory



P. Glatzel & U. Bergmann, Coord. Chem. Rev. (2005)

AGH Seminarium WFIIS, 24/01/2014

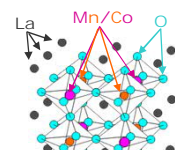
14

Spin state evolution in $\text{LaMn}_{1-x}\text{Co}_x\text{O}_3$ series

$\text{LaMn}_{1-x}\text{Co}_x\text{O}_3$ magnetoresistive perovskites

LaMnO_3 AFM insulator, orthorhombic, HS Mn^{3+} ($3d^4$, $S=2$)

LaCoO_3 diamagnetic, rhombohedral, LS Co^{3+} ($t_{2g}^6 e_g^0$, $S=0$)
spin excitations at $T > 90\text{K}$, $\langle S \rangle_{300\text{K}} \approx 0.5 - 1.2$

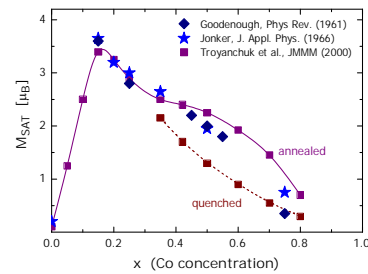


Solid solution

FM conducting, M_{SAT} up to $3.5\mu_B$
structural phase transition at $x \sim 0.6$
properties depend on synthesis route

Two possible origins of ferromagnetism:

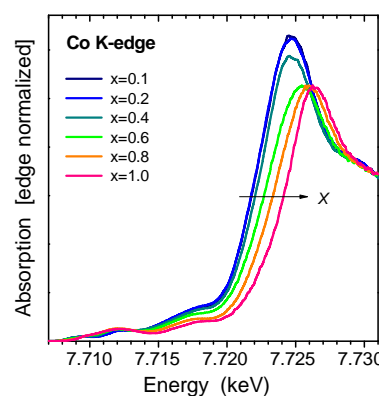
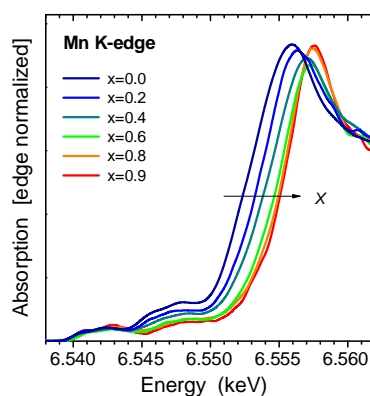
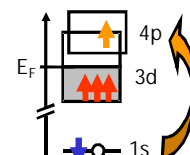
- homovalent substitution ($\text{Mn}^{3+}/\text{Co}^{3+}$),
 $\text{Mn}^{3+}-\text{O}-\text{Mn}^{3+}$ superexchange (SE) only
- $\text{Mn}^{4+}+\text{Co}^{2+}$ phase with surplus of either Mn^{3+} or Co^{3+}
set of SE and double-exchange (DE) interactions



$\text{LaMn}_{1-x}\text{Co}_x\text{O}_3$ series: K-edge XAS

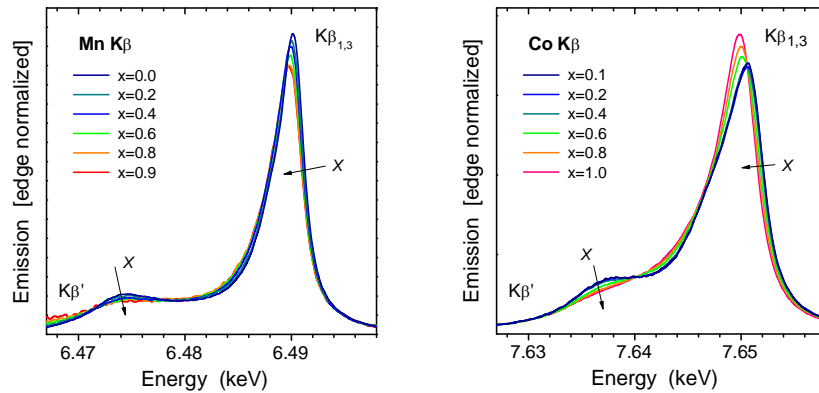
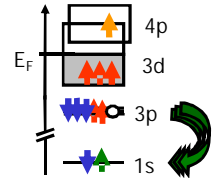
Shift of the edge position

- decrease of the effective charge and/or
- change in the 3d/4p hybridization (local structure evolution)
- both, Co and Mn edges, shift to the same direction
→ charge transfer



LaMn_{1-x}Co_xO₃ series: K β XES

- K $\beta_{1,3}$ and K β' lineshape
 → spectrum proportional to the 3d spin
 via 3d-3p exchange interaction
 → Co spectra reveal more pronounced evolution



AGH, Seminarium WFiIS, 24/01/2014

17

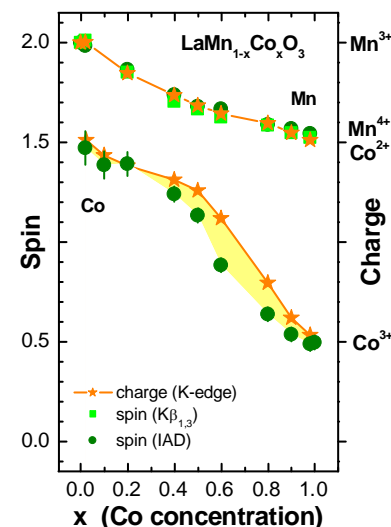
LaMn_{1-x}Co_xO₃ series: average Mn and Co spin

Spin derived indirectly using average charge estimation from K-edge XAS:

- HS only model for Mn ($S = n_{3d}/2$)
- mixed Co²⁺(HS)+Co³⁺(1/2) model for Co

Spin derived directly from K β XES by comparison to the reference samples:

- nice correlation for Mn → HS model confirmed
- significant difference in case of Co
 → average spin state lower than expected



AGH, Seminarium WFiIS, 24/01/2014

18

LaMn_{1-x}Co_xO₃ series: average Mn and Co spin

Spin derived from XAS:

- Co²⁺ ($S_{HS} = 3/2$) + Co³⁺ ($S_{LS} = 0$)

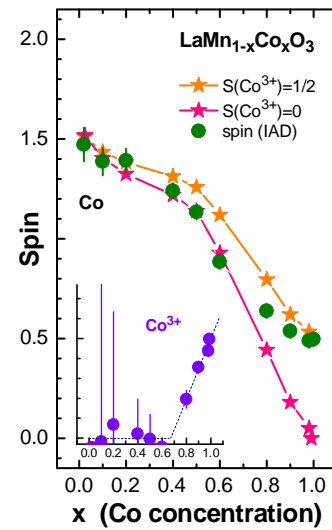
Spin derived directly from Kβ XES

- nice agreement at low and medium doping
- lack of correlation at high x

The explanation:

for $x > 0.6$ the average Co³⁺ spin at 300K rises gradually with x, coincides with structural phase transition at $x \sim 0.6$

Magnetic properties at high Co content depends on exact oxygen stoichiometry (Co³⁺ phase volume)



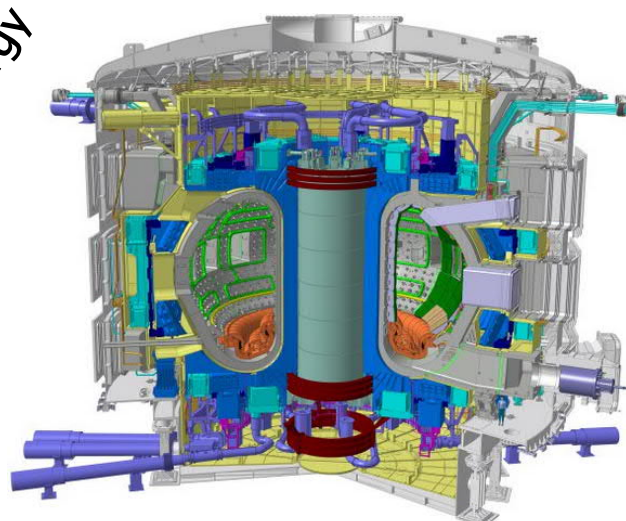
M.Sikora et al., J. Appl. Phys. 2008

AGH, Seminarium WFiIS, 24/01/2014

19

XAS-XES in „practical” applications

Thermonuclear energy

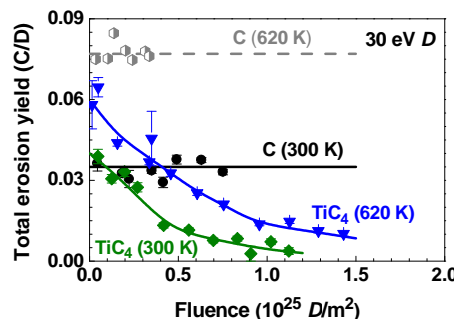


AGH, Seminarium WFiIS, 24/01/2014

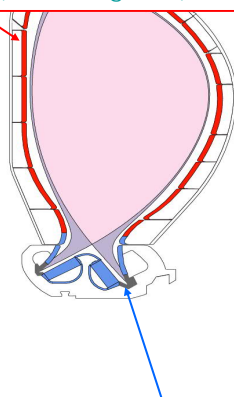
20

Plasma facing materials for ITER

- carbon fiber reinforced carbon (CFC)
 - can withstand the highest expected power without major degradation
 - good self-sputtering properties
 - chemical erosion by hydrogen**
 - reduced upon doping with transition metals



first wall: modest flux
Be (low Z, O getter)

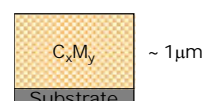
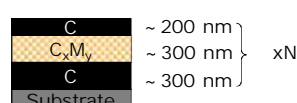


divertor wall: W
high heat flux 10 (20) MW/m²
target plates: C
transient heat loads (disruptions)

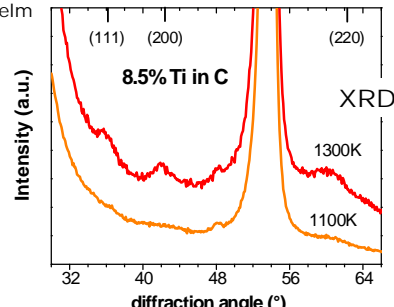
Metal doped carbon films

Courtesy of C. Adelhelm

Search for the best C_xM_y system in terms of resistance, self-sputtering and erosion combined with complete characterization



Best properties upon annealing at $T > 1100K$



RBS : good homogeneity

XRD : traces of crystallization

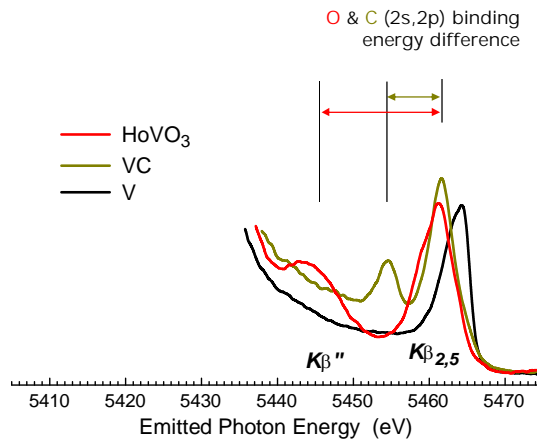
XPS : Very weak carbide-like spectrum upon annealing, traces of oxide & metallic phase in Ti samples

EXAFS : traces of non-carbide phases

K β satellite spectra

Oxygen and carbon K β'' peaks do not overlap

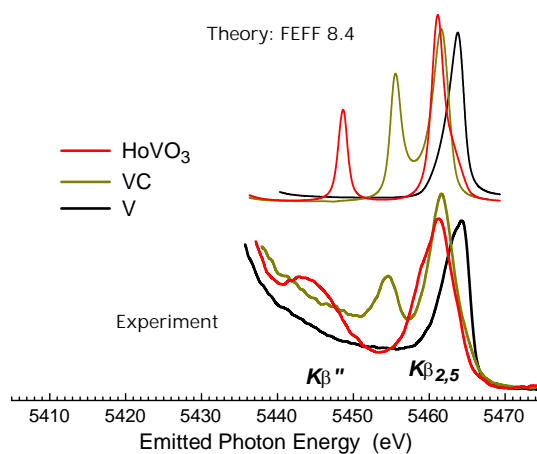
- K β'' and K $\beta_{2,5}$ intensity:
- is proportional to the number of ligands
 - depends on distance



K β satellite spectra

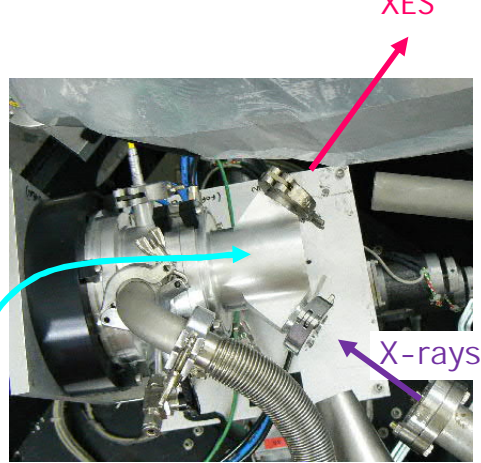
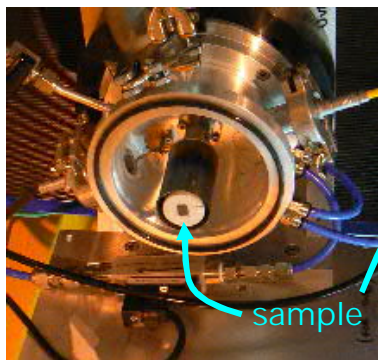
Oxygen and carbon K β'' peaks do not overlap

- K β'' and K $\beta_{2,5}$ splitting
- is nicely reproduced by theoretical calculations



In-situ XES at ID26 (ESRF, Grenoble)

Heating (cooling) speed: 3K/min
 Max. temperature: 1300K
 Ceramic heaters
 Controlled atmosphere



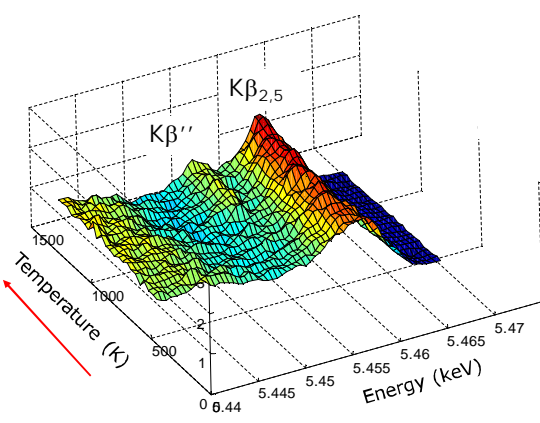
In-situ K β satellite spectra

Carbide formation at T~ 900K

Traces of V-O and V-C bonds
 in as deposited sample

Consistent with ex-situ

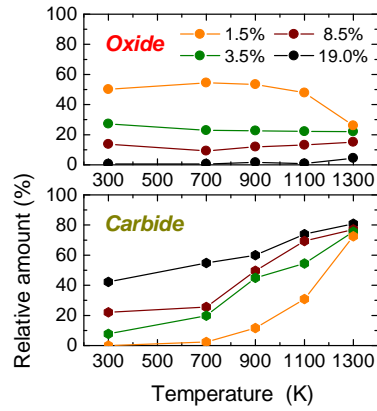
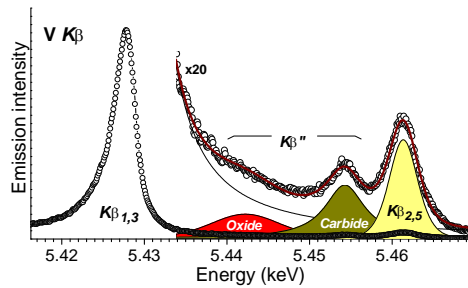
No changes upon cooling



Vanadium neighbourhood

Oxide is formed in 1.5% doped sample and released upon annealing at 1300K

Carbide phase increases with temperature and concentration



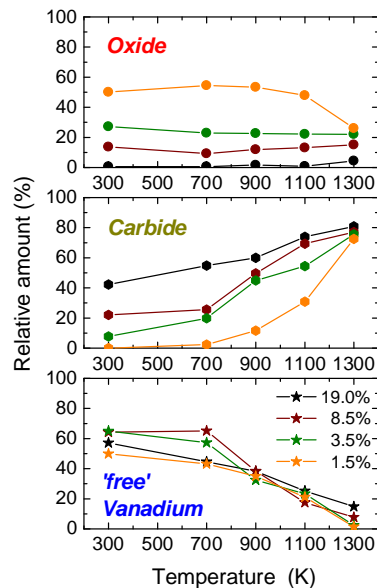
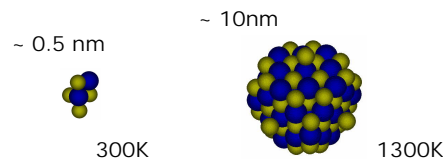
Vanadium neighbourhood

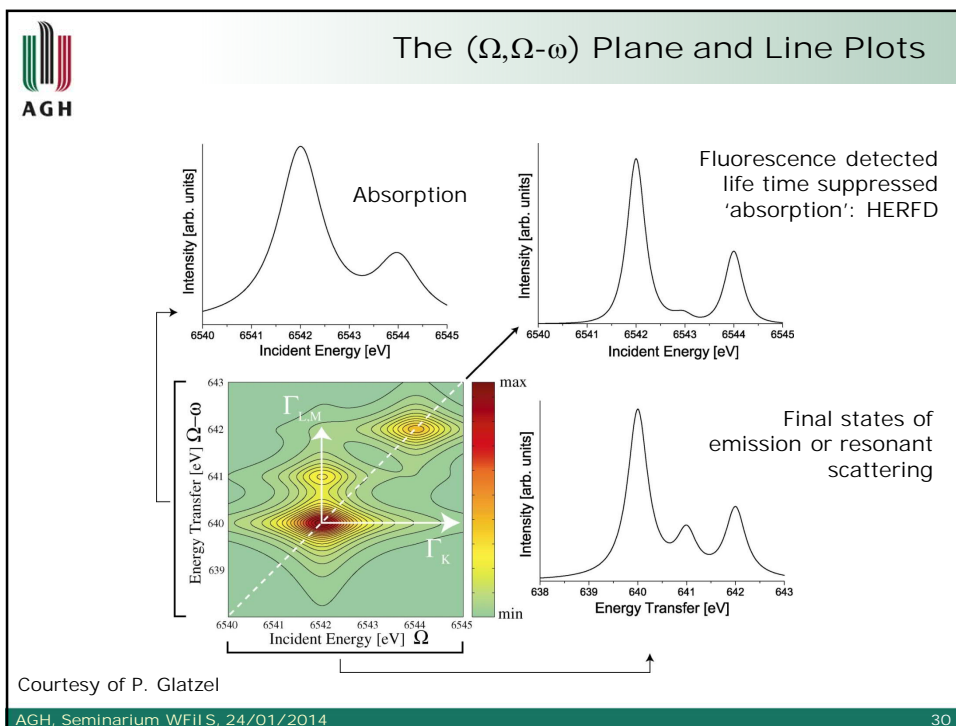
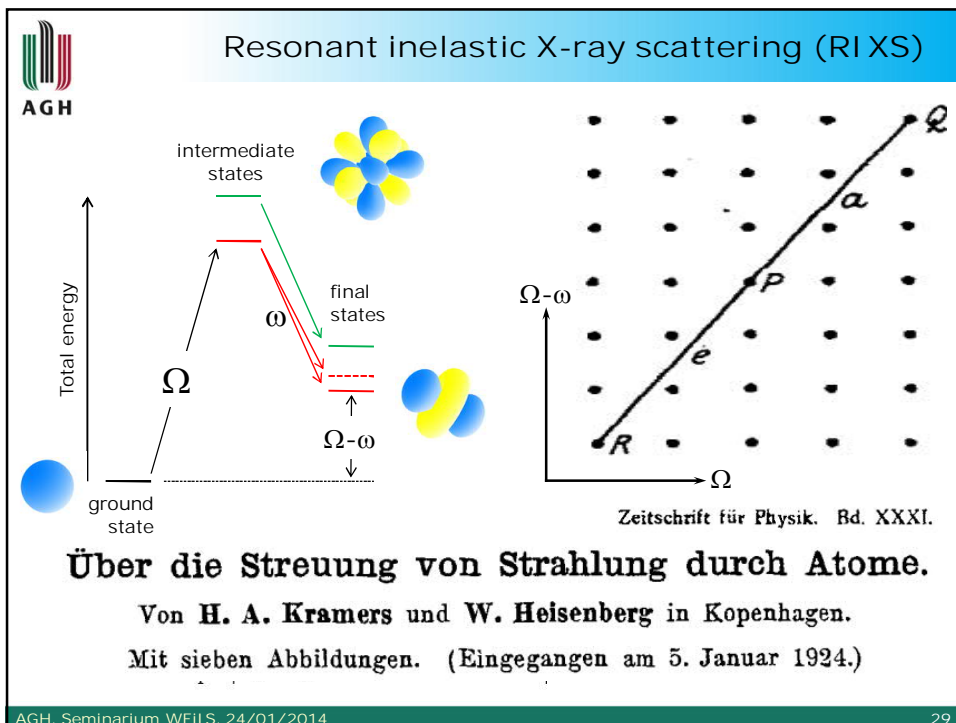
Oxide is formed in 1.5% doped sample and released upon annealing at 1300K

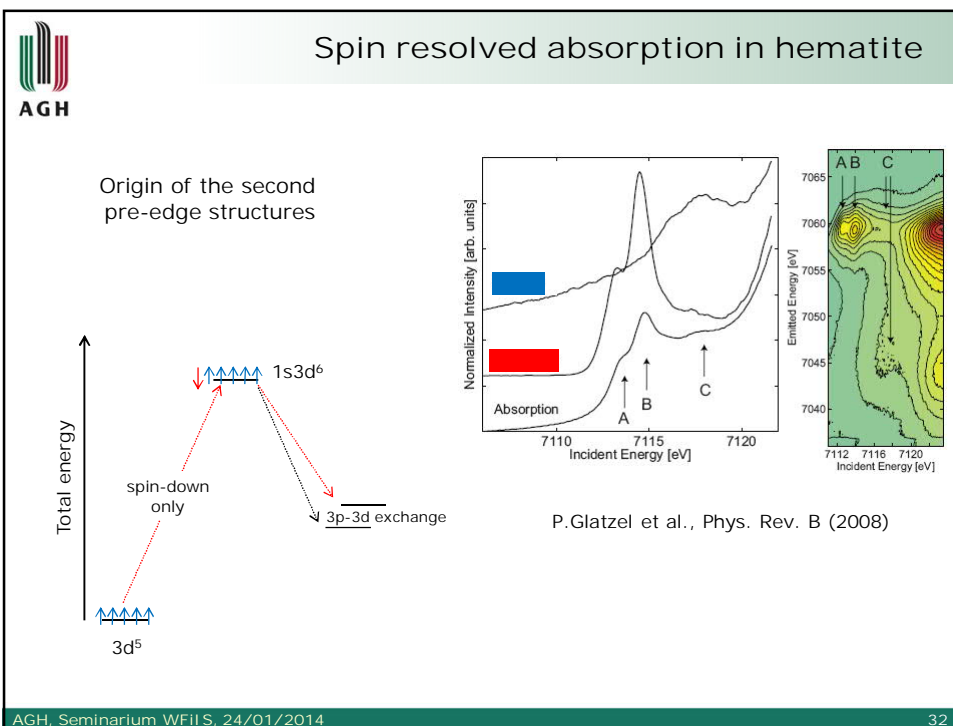
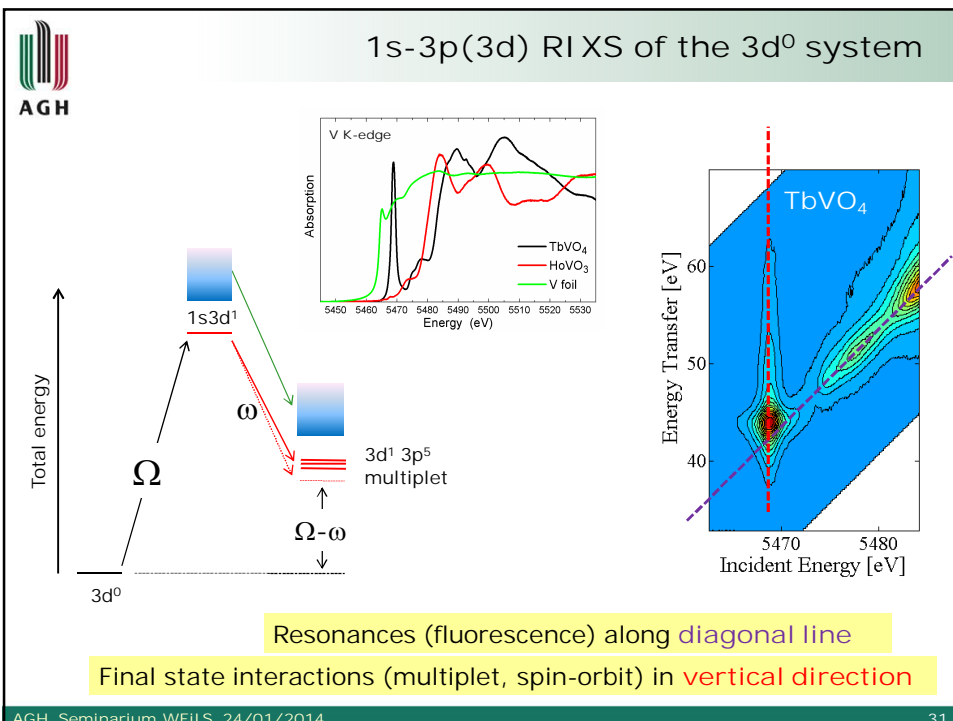
Carbide phase increases with temperature and concentration

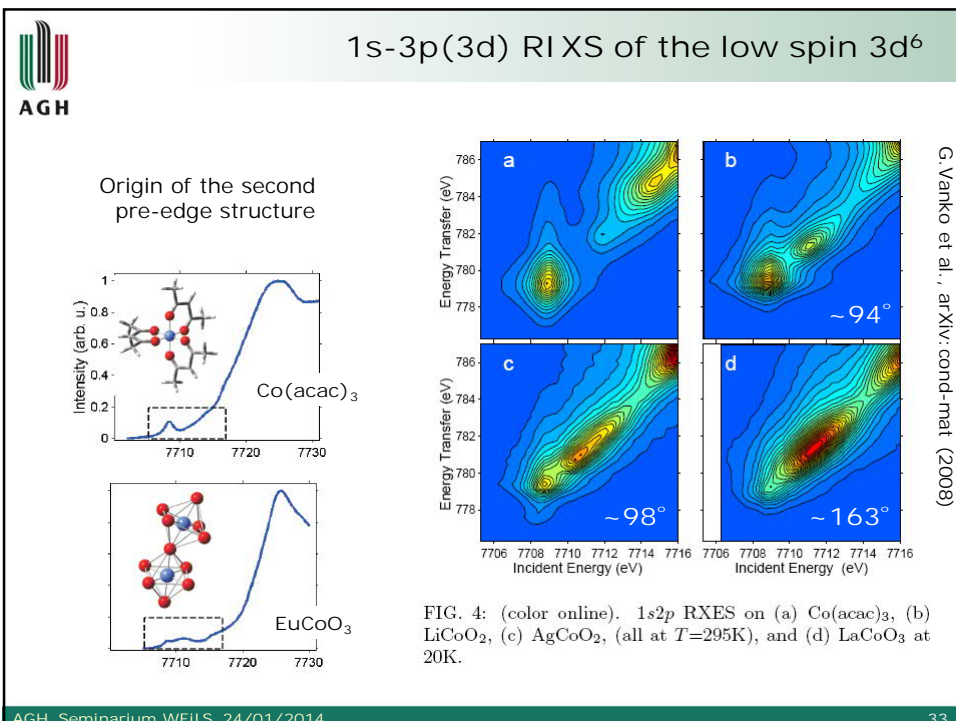
Amount of 'free' V bonds decreases from ~60% to ~10% upon annealing

Assuming VC (NaCl-like) structure, $d_{V-C} \approx 2\text{\AA}$, and taking surface/bulk ratio into account:



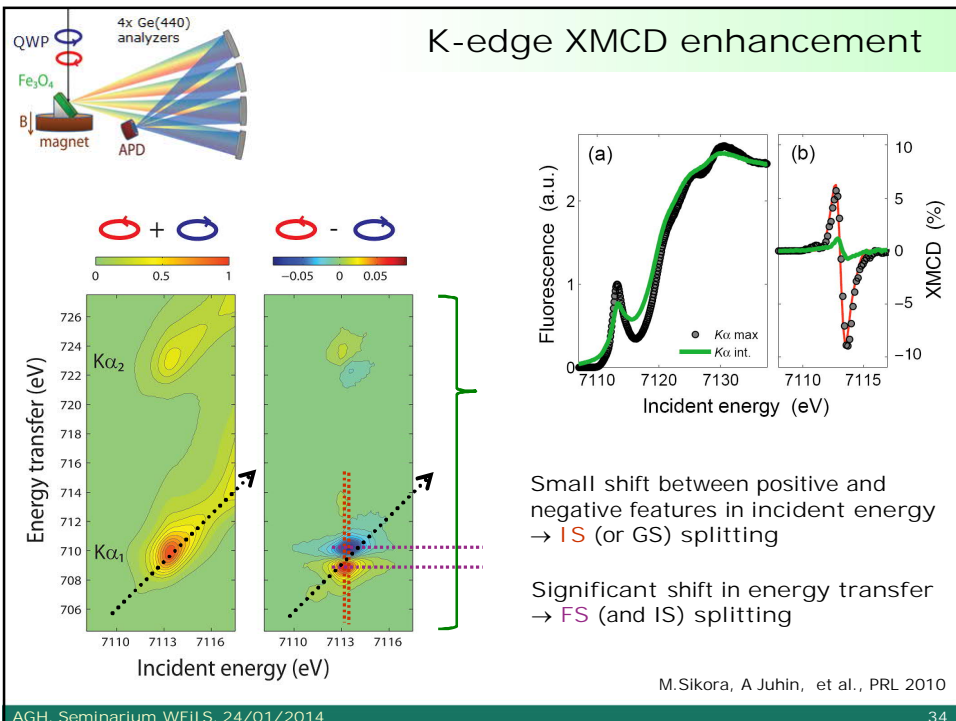






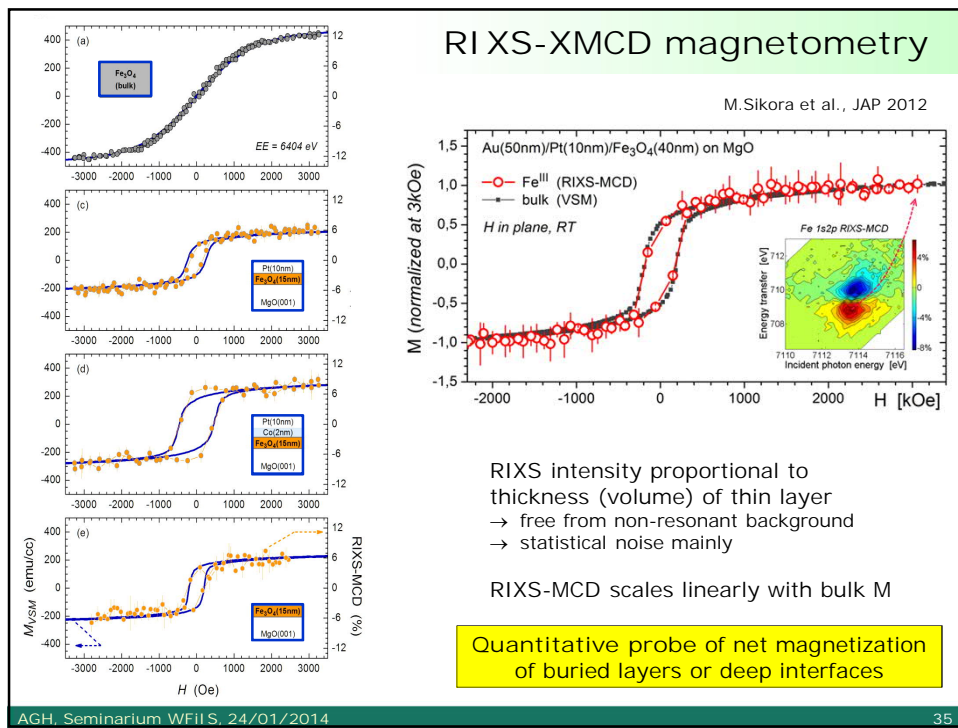
AGH Seminarium WFiS, 24/01/2014

33



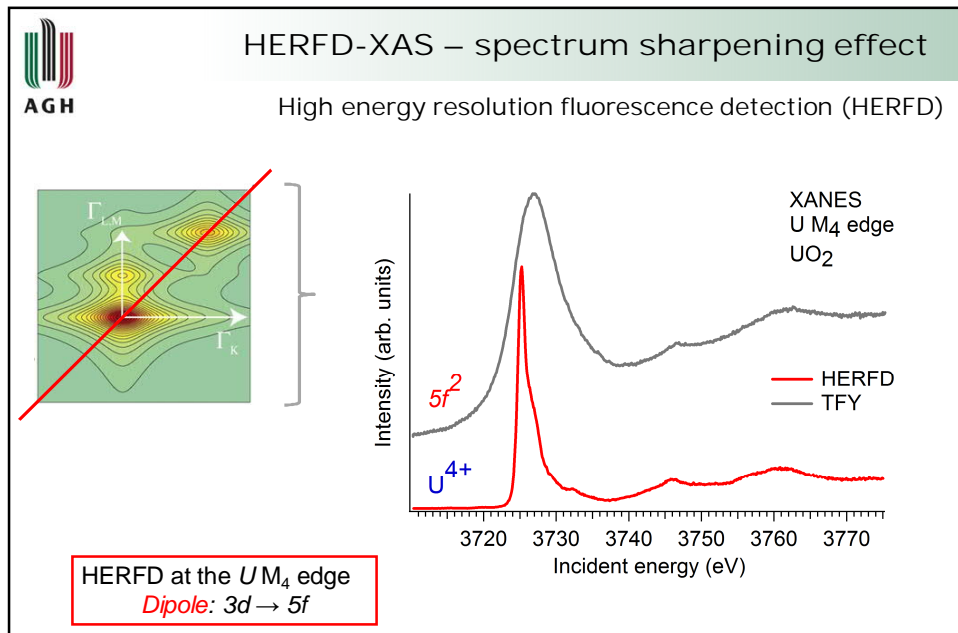
AGH Seminarium WFiS, 24/01/2014

34



AGH, Seminarium WFIIS, 24/01/2014

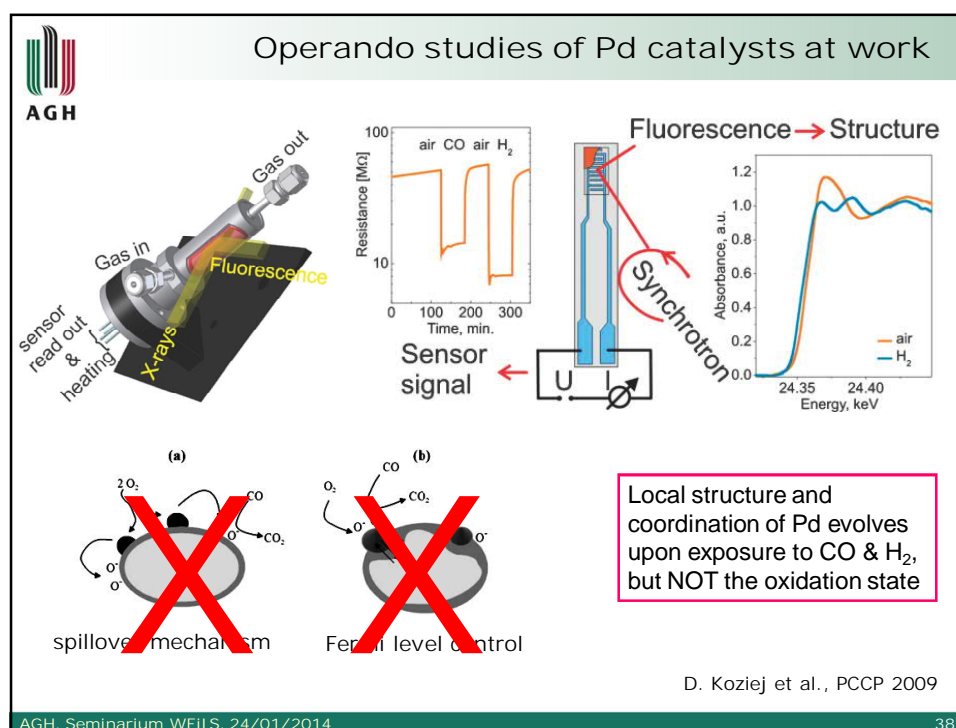
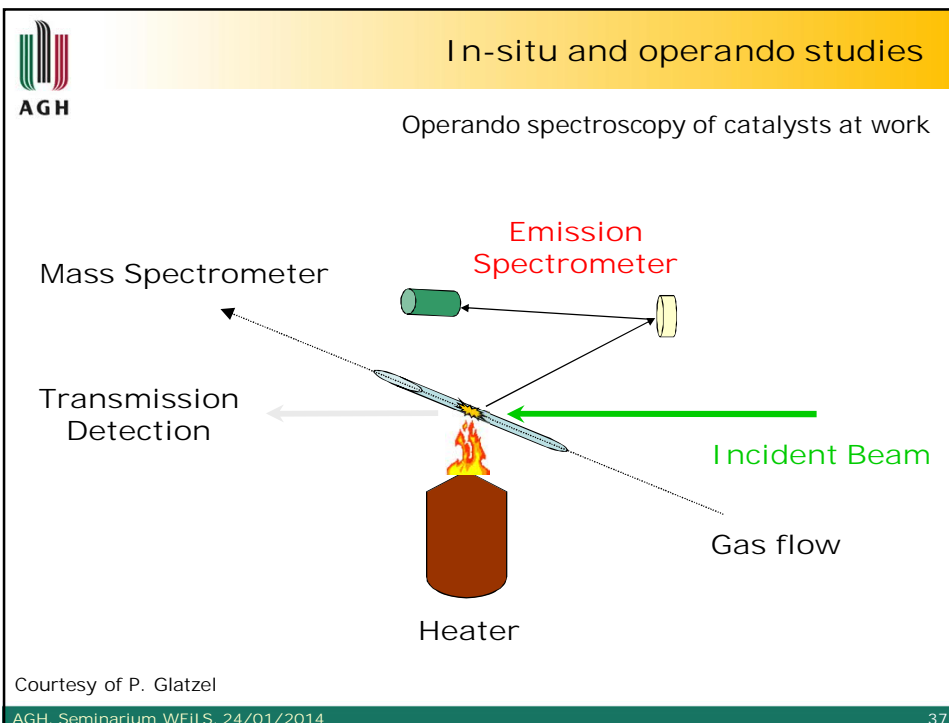
35



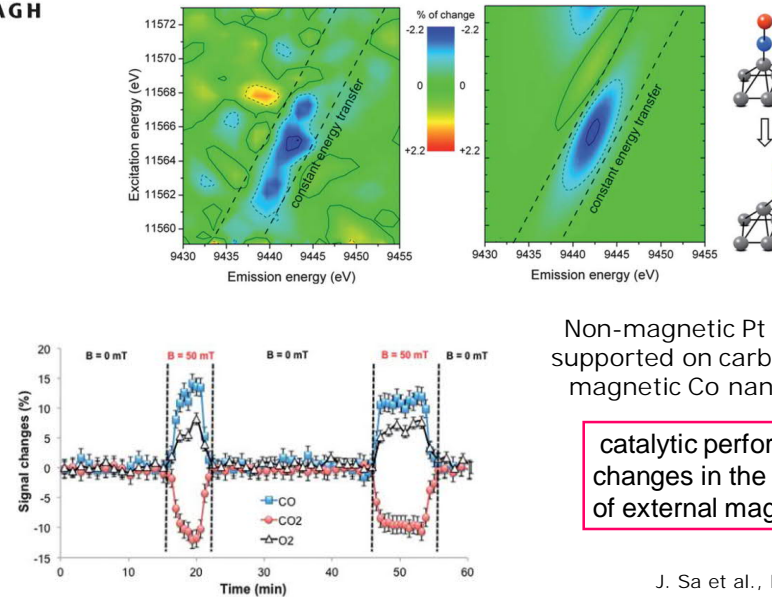
AGH, Seminarium WFIIS, 24/01/2014

K. Kvashnina et al., PRL 2013

36



Magnetic field controlled catalysis



J. Sa et al., *Nanoscale* 2013

AGH, Seminarium WFIIS, 24/01/2014

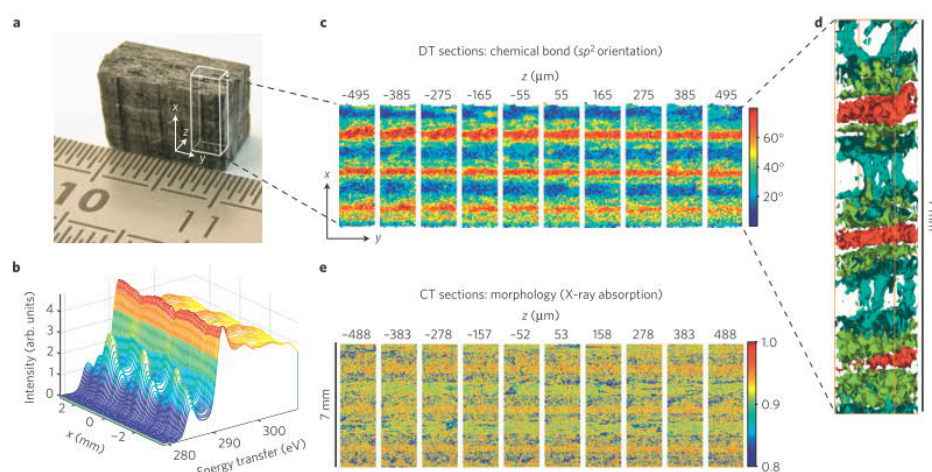
39

Direct tomography with chemical-bond contrast

Simo Huotari^{1,2*}, Tuomas Pylkkänen^{1,2}, Roberto Verbeni¹, Giulio Monaco¹ and Keijo Hämäläinen²

layered C/SiC

Nature Mat. 2011

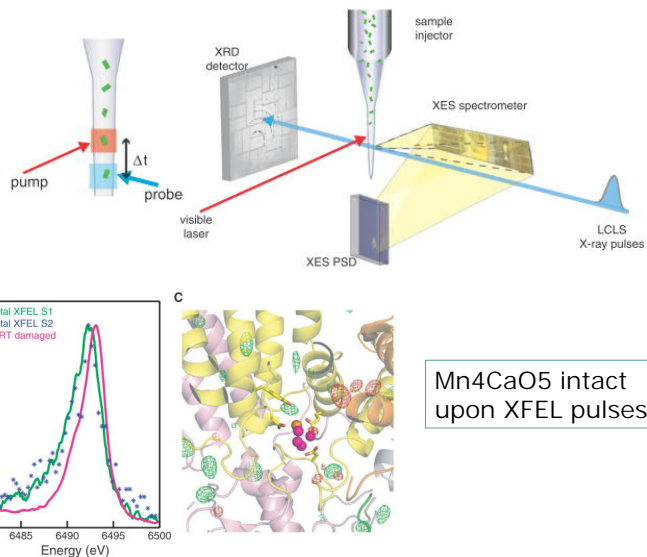


AGH, Seminarium WFIIS, 24/01/2014

40

Simultaneous Femtosecond X-ray Spectroscopy and Diffraction of Photosystem II at Room Temperature

Jan Kern et al.
Science 340, 491 (2013);
DOI: 10.1126/science.1234273



AGH, Seminarium WFIIS, 24/01/2014

41

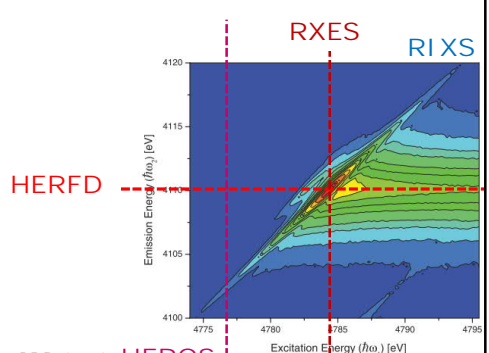
Why hard X-ray spectroscopy

Electronic and structural information

Element specific, symmetry sensitive
absorption edges, valence band emission

Compatible with extreme conditions
significant penetration depth

Number of
complementary
techniques
using same set-up:
XAS, XES,



M. Kavčič et al., PRB 2013 HEROS

AGH, Seminarium WFIIS, 24/01/2014

42